2014 IEEE International Conference on Robotics & Automation (ICRA)
Hong Kong Convention and Exhibition Center
May 31 - June 7, 2014. Hong Kong, China

Switching Control of Attitude Tracking on a Quadrotor UAV for Large-angle Rotational Maneuvers

Lu Wang and Jianbo Su

Abstract— **This paper studies an attitude tracking control system of a quadrotor unmanned aerial vehicle (UAV) under the condition of large-angle rotational maneuvers. We first established the attitude error model, taking both external disturbances and internal uncertainties into account. Thereafter, a switching control strategy is proposed for both high tracking accuracy and velocity constraints. Experiments on attitude tracking validate higher control accuracy with proposed method. Tasks of flight at unknown initial attitude and flip are also presented to verify the effectiveness of this method under large-angle rotational maneuverability.**

I. Introduction

Recently, quadrotor unmanned aerial vehicles (UAV) have attracted increasing interest in researches and applications in both military and civil society, such as unmanned inspection, rescue in disasters, and road traffic supervision.

Attitude tracking control of a quadrotor is the foundation of almost all the missions in this area. Various researches related to attitude controller design have been extensively studied based on several inspired approaches, such as feedback control [1,2], sliding mode control [3], adaptive control [4], nonlinear disturbance observer [5], neural networks [6], etc. Although some simulations and experiments are implemented successfully in these applications, the condition of large-angle rotational maneuverability is not considered. The attitude control under extreme maneuverability is investigated in [7,8]. However, only simulations are presented to validate the effectiveness of these methods. The flip of a quadrotor is implemented in several previous works [9-14]. The authors in [9-11] decouple the quadrotor model into a 2D model moving in a vertical plane and the out-of-plane dynamics, and the controller are designed respectively for the decoupled subsystems. In [11], the quadrotor is modeled as a collection of simplified hybrid modes, and reachability analysis guaranteeing safety and performance is implemented on a quadrotor for backflip maneuver. A motion planning and coordination strategy for robot systems based on representation space is investigated in [15]. Trajectory generation and control is also proposed on a quadrotor UAV for some special tasks such as minimum snap, obstacle avoidance, and suspended load [12-14].

Specifically, there are two prominent problems in the tracking control of quadrotor for large-angle rotational maneuvers: (i) attitude estimation and control method under large maneuvers; and (ii) state constraint for large tracking error or initial states error. In this paper, quaternion is introduced instead of Euler angles for attitude estimation and control. Then, system error model based on the attitude tracking problem is established. Consider the angular velocity constraint of the quadrotor, a practical switching control strategy is proposed for large-angle rotational maneuvers. When the system states are far away from the equilibrium point, we hope the systems converge to the equilibrium point with a bounded angular velocity. Hence, a controller with angular velocity constraint is designed. On the contrary, if the system states are close to the equilibrium point, a high accuracy of tracking performance is needed. At present, a tracking controller with a linear extended state observer (ESO) is proposed. A switching logic is presented based on a designed manifold. Experiments, such as attitude tracking, flight under unknown initial states and flip, are implemented on a quadrotor UAV testbed to validate the effectiveness of the proposed method.

This paper is organized as follows. In Section II, the system model of a quadrotor UAV based on quaternion is established. Then, attitude tracking problem with uncertainties is formulated. In Section III, two controllers under different conditions and a switching logic are proposed to compose a switching controller. In Section IV, experiments are carried out to verify the effectiveness of the proposed method, followed by Conclusions in Section V.

II. System Model and Problem Formulation

In the aforementioned works [2,4-6,9-14], the attitude of the quadrotor is described by Euler angles. However, its kinematics is not available when pitch angle $\theta = \pm\frac{\pi}{2}$. In this work, we choose quaternion to represent the attitude.

A. System Model

There are totally three coordinates used in this paper, earth frame $\mathcal{F}_e$, body-fixed frame $\mathcal{F}_b$, and orientated frame $\mathcal{F}_d$. The quadrotor is considered as a rigid body without deformation,

*This work was financially supported by Chinese National High-Tech Research and Development Program and National Natural Science Foundation of China (No. 60935001, 61221003).

[1]L. Wang and J. Su are with School of Electronic Information and Electric Engineering, Shanghai Jiao Tong University, Shanghai 200240, P.R. China. wanglu1987xy@sjtu.edu.cn; jbsu@sjtu.edu.cn

which is expressed in Fig. 1. The system model is described as [17]:

$$\begin{cases} \dot{q}_0 = -\frac{1}{2}\boldsymbol{q}^{\mathrm{T}}\boldsymbol{\omega}, \dot{\boldsymbol{q}} = \frac{1}{2}(q_0 I_3 + [\boldsymbol{q}\times])\boldsymbol{\omega} \\ J\dot{\boldsymbol{\omega}} = -\boldsymbol{\omega} \times J\boldsymbol{\omega} + F\boldsymbol{u}, \end{cases} \tag{1}$$

where q_0 and $\boldsymbol{q}$ are scalar and vector components of the unit quaternion, with $\boldsymbol{q} \in \mathcal{R}^3$ satisfying constraint $\boldsymbol{q}^{\mathrm{T}}\boldsymbol{q} + q_0^2 = 1$. $\boldsymbol{\omega} \in \mathcal{R}^3$ denotes the angular velocity of the rigid body, I_3 denotes the identity matrix with a dimension of three by three. Operator $[\cdot\times]$ denotes the skew-symmetric matrix of a vector. $J \in \mathcal{R}^{3\times3}$ is a symmetric positive definite constant inertia matrix. $\boldsymbol{u} \in \mathcal{R}^3$ is the control input of the rotational dynamics, F is a three-dimensional matrix where $F\boldsymbol{u}$ is the control torque of the quadrotor. We define the control input $\boldsymbol{u} = [\ \omega_\phi \quad \omega_\theta \quad \omega_\psi\ ]^{\mathrm{T}}$. Then, the rotational speeds of each propellers are:

$$\begin{cases} \omega_1 = \omega_T + \omega_\theta + \omega_\psi, \ \ \omega_2 = \omega_T + \omega_\phi - \omega_\psi \\ \omega_3 = \omega_T - \omega_\theta + \omega_\psi, \ \ \omega_4 = \omega_T - \omega_\phi - \omega_\psi. \end{cases} \tag{2}$$

where ω_1 is the corresponding speed of the rotor at north axis, and ω_2 to ω_4 are the speeds of last three rotors at the direction of counter-clockwise. ω_T is the speed of each rotor that enable the quadrotor at the state of hover.

From the principle of the quadrotor UAV, the control torque is shown as:

$$F\boldsymbol{u} = \begin{bmatrix} C_T\rho A r^2 l(\omega_1^2 - \omega_3^2) \\ C_T\rho A r^2 l(\omega_2^2 - \omega_4^2) \\ C_Q\rho A r^3(\omega_1^2 + \omega_3^2 - \omega_2^2 - \omega_4^2) \end{bmatrix}, \tag{3}$$

where C_T and C_Q are coefficients of thrust and torque from rotational speed, respectively. And ρ is density of air, r is propeller's radius, A is propeller's dics area, l is the rotor displacement from UAV center of mass. Assume that the value of $\boldsymbol{u}$ is smaller than that of ω_T, we finally get the matrix F as:

$$F = \mathrm{diag}(4C_T\rho A r^2 l\omega_T, 4C_T\rho A r^2 l\omega_T, 8C_Q\rho A r^3\omega_T). \tag{4}$$

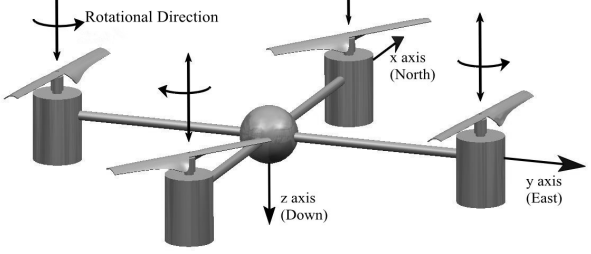

Fig. 1: Quadrotor UAV system.

B. Problem Formulation

Consider the attitude tracking problem of the quadrotor, we are trying to design a control input $\boldsymbol{u}$ to enable the quadrotor to track a desired attitude quickly and accurately. The vector $[\ \boldsymbol{q}_{\mathrm{d}} \quad \boldsymbol{\omega}_{\mathrm{d}} \quad \dot{\boldsymbol{\omega}}_{\mathrm{d}}\ ]$ represents the attitude information of the orientated frame $\mathcal{F}_d$, which contains desired quaternion, angular velocity, and angular acceleration. Also, the desired angular acceleration $\dot{\boldsymbol{\omega}}_{\mathrm{d}}$ is bounded.

The orthogonal attitude transition matrix is denoted by $R \in SO(3)$. The relative attitude and angular velocity variables from body frame $\mathcal{F}_b$ to the orientated frame $\mathcal{F}_d$ are defined as

$$\tilde{q}_0 = \tilde{q}_{0\mathrm{d}}\tilde{q}_0 + \boldsymbol{q}_{\mathrm{d}}^{\mathrm{T}}\boldsymbol{q}, \ \ \tilde{\boldsymbol{q}} = q_{0\mathrm{d}}\boldsymbol{q} - q_0\boldsymbol{q}_{\mathrm{d}} + \boldsymbol{q}\times\boldsymbol{q}_{\mathrm{d}}, \ \ \tilde{\boldsymbol{\omega}} = \boldsymbol{\omega} - \tilde{R}\boldsymbol{\omega}_{\mathrm{d}}, \tag{5}$$

where $\tilde{R} = RR_{\mathrm{d}}^{\mathrm{T}}$ is known as the error of attitude transition matrix. From the definition of $\tilde{\boldsymbol{\omega}}$, we get the following rotational error model as:

$$\begin{cases} \dot{\tilde{q}}_0 = -\frac{1}{2}\tilde{\boldsymbol{q}}^{\mathrm{T}}\tilde{\boldsymbol{\omega}}, \dot{\tilde{\boldsymbol{q}}} = \frac{1}{2}(\tilde{q}_0 I_3 + [\tilde{\boldsymbol{q}}\times])\tilde{\boldsymbol{\omega}} \\ \dot{\tilde{\boldsymbol{\omega}}} = J^{-1}[-(\tilde{\boldsymbol{\omega}} + \tilde{R}\boldsymbol{\omega}_{\mathrm{d}}) \times J(\tilde{\boldsymbol{\omega}} + \tilde{R}\boldsymbol{\omega}_{\mathrm{d}}) + F\boldsymbol{u}] \\ \quad - (\tilde{R}\dot{\boldsymbol{\omega}}_{\mathrm{d}} - [\tilde{\boldsymbol{\omega}}\times]\tilde{R}\boldsymbol{\omega}_{\mathrm{d}}). \end{cases} \tag{6}$$

Consider the model mismatch and external disturbances, we assume that the nominal inertia is J_0 and inertia error is defined as $\Delta J = J - J_0$. Also, the nominal value of F is given as F_0, and its error is defined as $\Delta F = F - F_0$. Then, we can use the feedback linearization:

$$\boldsymbol{u} = \boldsymbol{v} + F_0^{-1}L(\tilde{\boldsymbol{\omega}} + \tilde{R}\boldsymbol{\omega}_{\mathrm{d}})J_0^* + F_0^{-1}J_0(\tilde{R}\dot{\boldsymbol{\omega}}_{\mathrm{d}} - [\tilde{\boldsymbol{\omega}}\times]\tilde{R}\boldsymbol{\omega}_{\mathrm{d}}), \tag{7}$$

to reduce the system dynamics to:

$$\dot{\tilde{\boldsymbol{\omega}}} = J_0^{-1}F_0\boldsymbol{v} + J_0^{-1}F_0(\boldsymbol{d} + \boldsymbol{f}), \tag{8}$$

where the definition of the operator $L(\cdot)$ and superscript * satisfy $L(\tilde{\boldsymbol{\omega}} + \tilde{R}\boldsymbol{\omega}_{\mathrm{d}})J_0^* = (\tilde{\boldsymbol{\omega}} + \tilde{R}\boldsymbol{\omega}_{\mathrm{d}}) \times J_0(\tilde{\boldsymbol{\omega}} + \tilde{R}\boldsymbol{\omega}_{\mathrm{d}})$. Assume that the external disturbances $\boldsymbol{d}$ is bounded, $\boldsymbol{f}$ is the internal uncertainties. If we have $\delta \triangleq (FF_0)^{-1}(F_0\Delta J - \Delta F J_0)$, then

$$\boldsymbol{f} = -[\delta\dot{\tilde{\boldsymbol{\omega}}} + L(\tilde{\boldsymbol{\omega}} + \tilde{R}\boldsymbol{\omega}_{\mathrm{d}})\delta^* + \delta(\tilde{R}\dot{\boldsymbol{\omega}}_{\mathrm{d}} - [\tilde{\boldsymbol{\omega}}\times]\tilde{R}\boldsymbol{\omega}_{\mathrm{d}})]. \tag{9}$$

We will try to design a controller for the stabilization of the equilibrium point: $\tilde{\boldsymbol{q}} = 0, \tilde{\boldsymbol{\omega}} = 0$, with the existence of external disturbances and system uncertainties. From the orthogonality of transition matrix, we know $\tilde{R} = I_3$ when $\tilde{\boldsymbol{q}} = 0$. And from the orthogonality of attitude matrix, $\tilde{R} = I_3$ if and only if $R = R_{\mathrm{d}}$. Then, from the definition of $\tilde{\boldsymbol{\omega}}$, we get $\boldsymbol{\omega} = \boldsymbol{\omega}_{\mathrm{d}}$ while $\tilde{R} = I_3$ and $\tilde{\boldsymbol{\omega}} = 0$. This implies that stabilizing the error system in (6) is equivalent to the objective of attitude tracking control.

III. Switching Control Strategy Design

In the attitude tracking task, the actuators should provide the rigid body with control torque to enable the system states to converge to equilibrium point in state space. However, the

circumstances can be divided as the system states that are closed to or far away from the equilibrium point. For the first circumstance, the controller should process high-accurate tracking performance against the system uncertainties and external disturbances. Simultaneously, anti-windup of the angular velocity should be taken into account for the second circumstance, without consideration of system uncertainties.

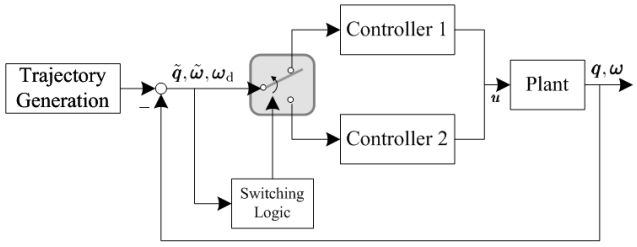

Fig. 2: Switching control framework.

From the analysis above, a practical switching control strategy is proposed for the attitude tracking task under condition of large-angle rotational maneuvers. The control structure is expressed in Fig. 2. There are two controllers to be designed for the two circumstances respectively. When the tracking error of the rigid body is large, we simplify the attitude tracking system into an attitude stabilization model, and velocity constraint is considered for the controller 1. For the other circumstance, a tracking controller with a linear ESO is proposed for high-accuracy [16]. The specified controllers and switching logic is given as follows.

A. Controller 1: Attitude stabilization with angular velocity constraints

Under the circumstance that the tracking error of the rigid body is large, the purpose of the controller is to stabilize the system states nearby the equilibrium point. In other words, we do not need this controller to stabilize the error model with high-accuracy, without consideration of system uncertainties. Thus, the controller can be designed based on the stabilization model.

If we set $\boldsymbol{\omega}_{\mathrm{d}} = 0$ and $\dot{\boldsymbol{\omega}}_{\mathrm{d}} = 0$, then Eq. (6) will be transformed to be an attitude stabilization model as:

$$\begin{cases} \dot{\tilde{q}}_0 = -\frac{1}{2}\tilde{\boldsymbol{q}}^{\mathrm{T}}\boldsymbol{\omega}, \dot{\tilde{\boldsymbol{q}}} = \frac{1}{2}(\tilde{q}_0 I_3 + [\tilde{\boldsymbol{q}}\times])\boldsymbol{\omega} \\ \dot{\boldsymbol{\omega}} = J^{-1}[-\boldsymbol{\omega}\times J\boldsymbol{\omega} + F\boldsymbol{u}]. \end{cases} \tag{10}$$

Then we define a Lyapunov function as:

$$\begin{aligned} V_1 = {} & \kappa_1 J^{-1}F[(1-\tilde{q}_0)^2 + \tilde{\boldsymbol{q}}^{\mathrm{T}}\tilde{\boldsymbol{q}}] \\ & + \frac{1}{2}(F_0^{-1}J_0)\ln\left[\prod_{i=0}^{3} w_i^2 / \prod_{i=0}^{3}(w_i^2-\omega_i^2)\right]. \end{aligned} \tag{11}$$

where κ_1 is a positive constant to be selected.

Here, the ln-term is introduced to guarantee $-w_i < \omega_i < w_i$ for $i = 1, 2, 3$ [17] and $w_i = 1.5rad/s$ is regarded as the upper bound of $|\omega_i|$. Then, we get the derivative of Lyapunov function V_1 as:

$$\dot{V}_1 = \kappa_1\tilde{\boldsymbol{q}}^{\mathrm{T}}(J^{-1}F)\boldsymbol{\omega} + \boldsymbol{\omega}^{\mathrm{T}}\Lambda\dot{\boldsymbol{\omega}}, \tag{12}$$

where $\Lambda = \mathrm{diag}\left(\frac{1}{w_1^2-\omega_1^2}, \frac{1}{w_2^2-\omega_2^2}, \frac{1}{w_3^2-\omega_3^2}\right)$.

Hence, a controller $\boldsymbol{u}_1$ could be designed as:

$$\boldsymbol{u}_1 = \Lambda^{-1}(-\kappa_1\tilde{\boldsymbol{q}} - \kappa_2\boldsymbol{\omega}). \tag{13}$$

where κ_2 is a positive constant to be designed.

Substituting Eq. (10) and (13) into Eq. (12), and notice that $\boldsymbol{\omega}^{\mathrm{T}}[\boldsymbol{\omega}\times] = 0$, we get:

$$\dot{V}_1 \le -\kappa_2\lambda_{\min}(J^{-1}F)\|\boldsymbol{\omega}\|^2. \tag{14}$$

Theorem 1. Given an attitude stabilization system of a quadrotor UAV expressed in Eq. (10) with angular velocity constraints, by applying the controller $\boldsymbol{u}_1$ in Eq. (13), we can come to a conclusion that the closed-loop system is asymptotically stable with $\lim_{t\to\infty}\tilde{\boldsymbol{q}} = 0$ and $\lim_{t\to\infty}\boldsymbol{\omega} = 0$.

Proof: This can be easily obtained by Barbalat's lemma and LaSalle's invariance principle.

B. Controller 2: Attitude tracking with linear ESO

The external disturbances and system uncertainties acting on the rotational dynamics will affect the performance of the control system, or even make the system unstable. The linear ESO treats these unknown properties as extended state to be estimated. Here, the total compound disturbance is defined as:

$$\boldsymbol{d}' = J_0^{-1}F_0(\boldsymbol{d} + \boldsymbol{f}). \tag{15}$$

Then, Eq. (8) can be rewritten as

$$\dot{\tilde{\boldsymbol{\omega}}} = J_0^{-1}F_0\boldsymbol{v} + \boldsymbol{d}', \dot{\boldsymbol{d}}' = \boldsymbol{h}(t), \tag{16}$$

where $\boldsymbol{h}(t)$ denotes the derivative of the compound disturbances $\boldsymbol{d}'$.

Then, the second-order linear ESO for (16) is proposed as:

$$\begin{cases} \dot{\hat{\boldsymbol{z}}}_1 = J_0^{-1}F_0\boldsymbol{v} + \hat{\boldsymbol{z}}_2 + g_1(\tilde{\boldsymbol{\omega}} - \hat{\boldsymbol{z}}_1) \\ \dot{\hat{\boldsymbol{z}}}_2 = g_2(\tilde{\boldsymbol{\omega}} - \hat{\boldsymbol{z}}_1), \end{cases} \tag{17}$$

where g_1 and g_2 are positive constants to be selected.

Converting Eq. (17) to the frequency-domain using the Laplace transform, and substitute Eq. (16) into (17), we get:

$$\begin{cases} s\hat{\boldsymbol{z}}_1 = (\hat{\boldsymbol{z}}_2 - \boldsymbol{d}') + s\tilde{\boldsymbol{\omega}} + g_1(\tilde{\boldsymbol{\omega}} - \hat{\boldsymbol{z}}_1) \\ s\hat{\boldsymbol{z}}_2 = g_2(\tilde{\boldsymbol{\omega}} - \hat{\boldsymbol{z}}_1), \end{cases} \tag{18}$$

where s is the Laplace operator.

From Eq. (18), we finally get

$$\hat{\boldsymbol{z}}_2 = \frac{g_2}{s^2 + g_1 s + g_2}\boldsymbol{d}'. \tag{19}$$

Selection of g_1 and g_2 should make the polynomial $s^2 + g_1 s + g_2$ to be Hurwitz. Here, we simply choose $g_2 = \omega_0^2, g_1 = 2\xi\omega_0$.

Then, we use the estimated disturbance of proposed linear ESO and design a torque input for the UAV that guarantees tracking of the desired quaternion. From the rotational error model, we know that the desired angular velocity and its time derivative should be used in the control law. These desired signals can be extracted by the kinematics of quaternion.

To design the attitude tracking controller, we introduce the following variable:

$$\tilde{\boldsymbol{\Omega}} = \tilde{\boldsymbol{\omega}} + k_1 \tilde{\boldsymbol{q}}, \tag{20}$$

and the control input $\boldsymbol{v}$ is designed as:

$$\begin{aligned} \boldsymbol{v} = &-(1 + k_1 k_2)\tilde{\boldsymbol{q}} - \left[k_2 + \frac{k_1^2}{2} F_0^{-1} J_0 (\tilde{q}_0 I_3 + [\tilde{\boldsymbol{q}}\times])\right]\tilde{\boldsymbol{\omega}} \\ &- F_0^{-1} J_0 \hat{\boldsymbol{z}}_2, \end{aligned} \tag{21}$$

where k_1 and k_2 are strictly positive constants.

From (7), the control torque of the attitude tracking problem is finally expressed as:

$$\begin{aligned} \boldsymbol{u}_2 = &-(1 + k_1 k_2)\tilde{\boldsymbol{q}} - (k_2 + \frac{k_1^2}{2} F_0^{-1} J_0 (\tilde{q}_0 I_3 + [\tilde{\boldsymbol{q}}\times])\tilde{\boldsymbol{\omega}} \\ &- F_0^{-1} J_0 \hat{\boldsymbol{z}}_2 + F_0^{-1} L(\tilde{\boldsymbol{\omega}} + \tilde{R}\boldsymbol{\omega}_{\mathrm{d}}) J_0^* \\ &+ F_0^{-1} J_0 (\tilde{R}\dot{\boldsymbol{\omega}}_{\mathrm{d}} - [\tilde{\boldsymbol{\omega}}\times]\tilde{R}\boldsymbol{\omega}_{\mathrm{d}}). \end{aligned} \tag{22}$$

Denote the estimating error of the linear ESO as $\tilde{\boldsymbol{d}}' \triangleq \boldsymbol{d}' - \hat{\boldsymbol{z}}_2$, then substitute Eq. (20) and (22) into Eq. (6):

$$\begin{cases} \dot{\tilde{q}}_0 = -\frac{1}{2}\tilde{\boldsymbol{q}}^{\mathrm{T}}(\tilde{\boldsymbol{\Omega}} - k_1\tilde{\boldsymbol{q}}), \dot{\tilde{\boldsymbol{q}}} = \frac{1}{2}(\tilde{q}_0 I_3 + [\tilde{\boldsymbol{q}}\times])(\tilde{\boldsymbol{\Omega}} - k_1\tilde{\boldsymbol{q}}) \\ F_0^{-1} J_0 \dot{\tilde{\boldsymbol{\Omega}}} = -\tilde{\boldsymbol{q}} - k_2\tilde{\boldsymbol{\Omega}} + F_0^{-1} J_0 \tilde{\boldsymbol{d}}'. \end{cases} \tag{23}$$

A Lyapunov function is defined as:

$$V_2 = [(1 - \tilde{q}_0)^2 + \tilde{\boldsymbol{q}}^{\mathrm{T}}\tilde{\boldsymbol{q}}] + \frac{1}{2}\tilde{\boldsymbol{\Omega}}^{\mathrm{T}}(F_0^{-1} J_0)\tilde{\boldsymbol{\Omega}}. \tag{24}$$

Then, we get the derivative of Lyapunov function V_2 as:

$$\dot{V}_2 \le -k_1\|\tilde{\boldsymbol{q}}\|^2 - k_2\|\tilde{\boldsymbol{\Omega}}\|^2 + \lambda_{\max}(F_0^{-1} J_0)\|\tilde{\boldsymbol{\Omega}}\|\|\tilde{\boldsymbol{d}}'\|. \tag{25}$$

Assume the estimating error of linear ESO as the input of the above system. Hence, the unforced form of system (23) is uniformly asymptotically stable at the equilibrium point. Then we analyze the stability of the overall system with ESO.

Theorem 2. Given a rotational error system of a quadrotor UAV in (6) for a desired attitude trajectory defined as $[\ \boldsymbol{q}_{\mathrm{d}} \quad \boldsymbol{\omega}_{\mathrm{d}} \quad \dot{\boldsymbol{\omega}}_{\mathrm{d}}\ ]$. With the external disturbances $\boldsymbol{d}$ and internal uncertainties $\boldsymbol{f}$ in (9), let the linear ESO expressed by (17) and the nonlinear feedback controller defined by (22). The quaternion error $\tilde{\boldsymbol{q}}$, angular velocity error $\tilde{\boldsymbol{\omega}}$, and estimation error $\tilde{\boldsymbol{d}}'$ of linear ESO are uniformly ultimately bounded (UUB).

Proof. From Eq. (19), we get

$$\tilde{\boldsymbol{d}}' = \frac{s^2 + g_1 s}{s^2 + g_1 s + g_2}\boldsymbol{d}', \tag{26}$$

then the state space realization of linear ESO can be represented as

$$\begin{cases} \dot{\boldsymbol{x}} = A\boldsymbol{x} + B\boldsymbol{d}' \\ \tilde{\boldsymbol{d}}' = C\boldsymbol{x} + D\boldsymbol{d}', \end{cases} \tag{27}$$

where $A = \begin{bmatrix} 0 & -g_2 \\ 1 & -g_1 \end{bmatrix}$, $B = \begin{bmatrix} -g_2 \\ 0 \end{bmatrix}$, $C = [\ 0 \quad 1\ ]$, $D = 1$. Notice that $\det(sI_3 - A) = s^2 + g_1 s + g_2$, which means A is Hurwitz if g_1 and g_2 are well-selected. That is, for any given positive definite symmetric matrix Q, there exists a positive definite symmetric matrix P that satisfies: $PA + A^{\mathrm{T}}P = -Q$.

From Assumption 1, the external disturbances $\boldsymbol{d}$ is bounded. Here, we focus on the expression of $\boldsymbol{f}$. Notice that all the variables are bounded except $\tilde{\boldsymbol{\omega}}$, we conclude that the following inequality is satisfied for positive a_1 to a_3.

$$\|\boldsymbol{d}'\| \le a_1\|\tilde{\boldsymbol{\Omega}}\| + a_2\|\tilde{\boldsymbol{\Omega}}\|^2 + a_3. \tag{28}$$

Then, we define a new Lyapunov function $V = V_2 + \frac{1}{2}\boldsymbol{x}^{\mathrm{T}}P\boldsymbol{x}$, the derivative of V is given as:

$$\begin{aligned} \dot{V} \le &-k_1\|\tilde{\boldsymbol{q}}\|^2 - k_2\|\tilde{\boldsymbol{\Omega}}\|^2 + \lambda_{\max}(F_0^{-1} J_0)\|\tilde{\boldsymbol{\omega}}\|\|\tilde{\boldsymbol{d}}'\| \\ &- \lambda_{\min}(Q)\|\boldsymbol{x}\|^2 + 2\lambda_{\max}(P)\lambda_{\max}(B)\|\boldsymbol{x}\|\|\tilde{\boldsymbol{d}}'\|. \end{aligned} \tag{29}$$

Substituting (28) into (29), yields:

$$\dot{V} \le -k_1\|\tilde{\boldsymbol{q}}\|^2 - c_1\|\tilde{\boldsymbol{\Omega}}\|^2 - c_2\|\boldsymbol{x}\|^2 + \mu, \tag{30}$$

where

$$\begin{aligned} c_1 = &k_2 - a_1\lambda_{\max}(F_0^{-1} J_0) - \frac{\lambda_{\max}(F_0^{-1} J_0)\lambda_{\max}(C)}{2\lambda_1} \\ &- a_2\lambda_{\max}(F_0^{-1} J_0)\|\tilde{\boldsymbol{\Omega}}\| - \frac{[a_3\lambda_{\max}(F_0^{-1} J_0)]^2}{4\mu_1} \\ &- \frac{a_1\lambda_{\max}(P)\lambda_{\max}(B)}{\lambda_2} - \frac{a_2\lambda_{\max}(P)\lambda_{\max}(B)}{\lambda_3}\|\tilde{\boldsymbol{\Omega}}\|^2, \end{aligned}$$

$$\begin{aligned} c_2 = &\lambda_{\min}(Q) - \frac{\lambda_1\lambda_{\max}(F_0^{-1} J_0)\lambda_{\max}(C)}{2} \\ &- a_1\lambda_2\lambda_{\max}(P)\lambda_{\max}(B) - a_2\lambda_3\lambda_{\max}(P)\lambda_{\max}(B) \\ &- \frac{[a_3\lambda_{\max}(P)\lambda_{\max}(B)]^2}{\mu_2}, \end{aligned}$$

$$\mu = \mu_1 + \mu_2.$$

where λ_i and μ_i are all positive constant.

Assume that Ω_0 is the upper bound of $\tilde{\boldsymbol{\Omega}}$ that makes $c_1 > 0$. For the original $\|\tilde{\boldsymbol{\Omega}}(t_0)\| < \Omega_0$, we find that $\dot{V}$ is strictly negative provided that the following inequalities hold: $\|\tilde{\boldsymbol{q}}\| > \sqrt{\frac{\mu}{k_1}}$, or $\|\tilde{\boldsymbol{\Omega}}\| > \sqrt{\frac{\mu}{c_1}}$, or $\|\tilde{\boldsymbol{d}}\| > \sqrt{\frac{\mu}{c_2}}$. Then, it can be concluded that the above three states are UUB and can converge into a compact set. Notice that $(\tilde{\boldsymbol{q}}, \tilde{\boldsymbol{\Omega}})$ are linear diffeomorphism of $(\tilde{\boldsymbol{q}}, \tilde{\boldsymbol{\omega}})$. Hence, $(\tilde{\boldsymbol{q}}, \tilde{\boldsymbol{\omega}})$ can converge into a compact set. Finally, we can come to a conclusion that the quaternion error, angular velocity error, and estimation error of linear ESO are UUB.

C. Switching Logic

If the tracking error of the system is large, controller 1 should be used to make the system states converge to equilibrium point quickly. However, when the system states are close to the desired attitude trajectory, the system should be switched to controller 2 for higher tracking accuracy. Here, a manifold is defined as $S = \tilde{\boldsymbol{q}} + k\tilde{\boldsymbol{\omega}}$. The switching condition is given as:

$$\begin{cases} \text{If}: \quad |S| > S_0, \text{Controller 1} \\ \text{Else if}: \quad |S| \leq S_0, \text{Controller 2} \end{cases} \tag{31}$$

where S_0 is a positive constant to be determined. k is a positive constant defined as 5.5. S_0 is selected as 0.3. The larger S_0 is selected, the more Controller 1 will be switched.

By the defined manifold, not only the attitude error, but also the angular velocity error are taken into account in the switching logic. If the switching of these two controllers is only determined by the attitude tracking error, the following two situations may be occurred. First, if the attitude error is small, however the angular velocity error is large, the attitude stabilization controller should be used. Then, the attitude error is large while the rigid body is converging to the equilibrium point quickly with a large angular velocity error, the controller system should be switched to tracking controller. However, if only attitude tracking error is used, the optimal controller cannot be switched under these two conditions. Consequently, both attitude error and the speed of rigid body converges to the equilibrium point will be considered in the switching logic.

The switching between the proposed controllers may lead the system unstable. We should consider the stability of the overall system with switching logic. Since controller 2 is locally UUB, as soon as controller 1 can stabilize the system states into the region of attraction of controller 2 with specified parameters, then we can conclude that the overall switching system is stable.

IV. Flight Test

Three experiments have been conducted to verify the proposed methods in this paper. The attitude tracking case is presented in the first experiment to show the high accuracy of control performance. Then, two tasks of flight at unknown initial attitude and flip are carried out to validate the controller's performance under large-angle rotational maneuvers. Our experimental platform is shown in Fig. 3. The mechanical structure of the UAV is based on the material of carbon fiber. For the elaboration of the real-time flight control (FC) board, it consists of a micro-processor, an IMU and an electronic compass. The IMU provides us with digital signal of three-axis angular velocities and accelerations. The electronic compass gives the three-axis magnetic of the rigid body. The micro-processor is used to capture the signal data from the sensors and to implement the control strategy.

Fig. 3: Quadrotor testbed.

A. Attitude tracking

An attitude tracking mission is accomplished, while the desired attitude is expressed as follows:

$$\boldsymbol{q}_{\mathrm{d}1} = 0.1\cos(\frac{\pi}{15}t), \ \boldsymbol{q}_{\mathrm{d}2} = 0.1\sin(\frac{\pi}{15}t), \ \boldsymbol{q}_{\mathrm{d}3} = 0. \tag{32}$$

A load disturbance of $0.0388N \cdot m$ in pitch and roll torque is introduced respectively to validate the disturbance rejection ability and robustness of the designed controller and linear ESO. The tracking effect is shown in Fig. 4.

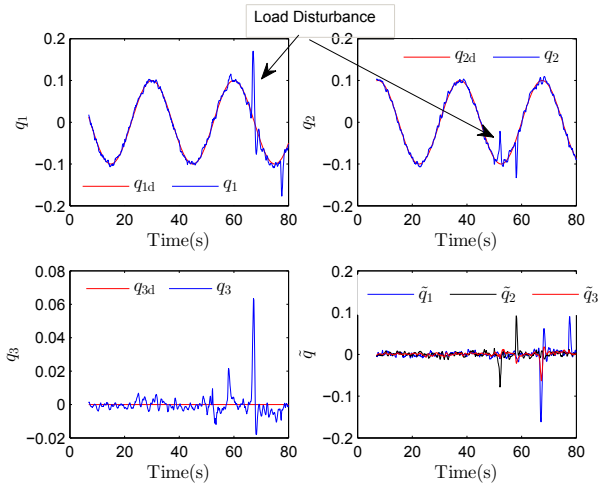

Fig. 4: Attitude tracking performance.

In Fig. 4, we find that with the action of linear ESO, the quaternion tracking error can be limited into 0.005 (about 0.3° of Euler angles). Also, at time of 52 and 67 seconds, external disturbances on the quadrotor are exerted. The linear ESO can eliminate the disturbance quickly and accurately with its convergence time less than 2 seconds.

B. Tasks under large-angle rotational maneuvers

The tasks of flight at unknown initial states and flip are carried out and shown in Figs. 5 and 6. The proposed switching

strategy is useful for large-angle rotational maneuvers.

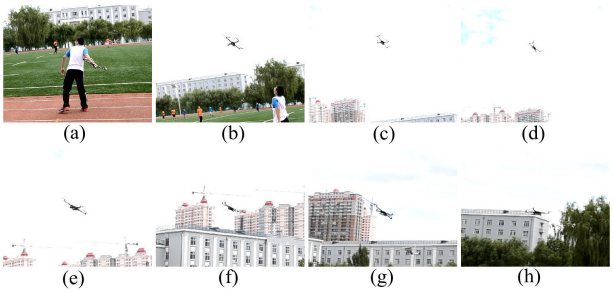

Fig. 5: Task of flight at unknown attitude. (a)-(d) A quadrotor is thrown out and in free fall. (e) The actuators are turning on. (f)-(g) Adjustment of the quadrotor. (h) Stabilization.

Fig. 6: Task of flip.

It is shown in Fig. 5 that the proposed controller can stabilize a quadrotor with large-angle rotational maneuvers without overshot. When the initial attitude error is large, the controller is switched into the attitude stabilization controller with angular velocity constraints. Hence, the attitude of the quadrotor can converge to equilibrium point with a bounded angular velocity, which restrain the appearance of overshot. Fig. 6 shows the whole process of the flipping task of a quadrotor. When the flipping command is given to the quadrotor, the controller will generate a large quaternion. Then, the controller will switching into Controller 1, which will enable the quadrotor to rotate at a constant speed w_i. At last, when attitude of the quadrotor changes nearby the equilibrium point, the controller switches into Controller 2 to extract high control accuracy. From the experiments, it is shown that the proposed control strategy can adapt to different condition in the work space, and also, it can acquire high-accuracy tracking performance against uncertainties.

V. Conclusion

In this paper, the design and implementation of a switching control strategy on a quadrotor UAV is proposed for large-angle rotational maneuvers. With the establishment of attitude error model, a switching control strategy is proposed for both higher tracking accuracy and requirement of velocity constraint. Three experiments have been carried out on a quadrotor testbed. The result of attitude tracking shows that the proposed method can make a quadrotor UAV to track a desired attitude quickly and accurately, with the tracking error being limited within $\pm 0.3^\circ$. The remaining two experiments indicate that the switching controller is well-designed for circumstance of large-angle rotational maneuvers.

References

[1] A. Tayebi, S. McGivray, *Attitude stabilization of a VTOL quadrotor aircraft*, IEEE Trans. Control Syst. Technol., vol. 14, no. 3, pp. 562–571, 2006.

[2] I. González, S. Salazar, J. Torres, R. Lozano, *Real-Time Attitude Stabilization of a Mini-UAV Quad-rator Using Motor Speed Feedback*, J. Intell. Robot. Syst., vol. 70, no. 1-4, pp. 93–106, 2013.

[3] L. Wang, H. Jia, *The Trajectory Tracking Problem of Quadrotor UAV: Global Stability Analysis and Control Design Based on the Cascade Theory*, Asian J. Control, vol. 16, no. 2, pp. 1-15, 2014.

[4] C. Nicol, C. J. B. Macnab, A. Ramirez-Serrano, *Robust adaptive control of a quadrotor helicopter*, Mechatronics, vol. 21, no. 6, pp. 927–938, 2011.

[5] C. Liu, W. H. Chen, J. Andrews, *Tracking control of small-scale helicopters using explicit nonlinear MPC augmented with disturbance observers*, Control Eng. Practice, vol. 20 no. 3, pp. 258–268, 2012.

[6] M. O. Efe, *Neural network assisted computationally simple control of a quadrotor UAV*, IEEE Trans. on Ind. Inform., vol. 7, no. 2, pp. 354–361, 2011.

[7] T. Lee, *Exponential stability of an attitude tracking control system on SO (3) for large-angle rotational maneuvers*, Syst. Control Lett., vol. 61, no. 1, pp. 231–237, 2012.

[8] I. Ali, G. Radice, J. Kim, *Backstepping control design with actuator torque bound for spacecraft attitude maneuver*, J. Guid. Control Dyn., vol. 33, no. 1, pp. 254–259, 2010.

[9] S. Lupashin, A. Schöllig, M. Sherback, *A simple learning strategy for high-speed quadrocopter multi-flips*, In Proc. of the IEEE Int. Conf. on Robotics and Automation, Anchorage, AK, pp. 1642–1648, May 2010.

[10] J. H. Gillula, H. Huang, M. P. Vitus, C. J. Tomlin, *Design of guaranteed safe maneuvers using reachable sets: Autonomous quadrotor aerobatics in theory and practice*, In Proc. of the IEEE Int. Conf. on Robotics and Automation, Anchorage, AK, pp. 1649–1654, May 2010.

[11] J. H. Gillula, G. H. Hoffmann, H. Huang, M. P. Vitus, C. J. Tomlin, *Applications of hybrid reachability analysis to robotic aerial vehicles*, The Int. J. Robot. Research, vol. 30, no. 3, pp. 335–354, 2011.

[12] D. Mellinger, V. Kumar, *Minimum snap trajectory generation and control for quadrotors*, In Proc. of the IEEE Int. Conf. on Robotics and Automation, Shanghai, China, pp. 2520–2525, May 2011.

[13] D. Mellinger, A. Kushleyev, V. Kumar, *Mixed-integer quadratic program trajectory generation for heterogeneous quadrotor teams*, In Proc. of the IEEE Int. Conf. on Robotics and Automation, Saint Paul, MN, pp. 477–483, May 2012.

[14] K. Sreenath, N. Michael, V. Kumar, *Trajectory Generation and Control of a Quadrotor with a Cable-Suspended Load A Differentially-Flat Hybrid System*, In Proc. of the IEEE Int. Conf. on Robotics and Automation, to appear, May 2013.

[15] J. Su, W. Xie, *Motion Planning and Coordination for Robot Systems Based on Representation Space*, IEEE Trans. Syst., Man, Cybern. B, Cybern., vol. 41, no. 1, pp. 248-259, 2011.

[16] Q. Zheng, L. Dong, D. H. Lee, Z. Gao, *Active Disturbance Rejection Control for MEMS Gyroscopes*, IEEE Trans. Ind. Electron., vol. 17, no. 6, pp. 1432–1438, 2009.

[17] Q. Hu, B. Li, Y. Zhang, *Robust attitude control design for spacecraft under assigned velocity and control constraints*, ISA Trans., vol. 52, no. 4, pp. 480-493, 2013.